

PROGRESS WITH BUNCH-SHAPE MEASUREMENTS AT PSI'S HIGH-POWER CYCLOTRONS AND PROTON BEAM LINES

R. Dölling, Paul Scherrer Institute, Villigen, Switzerland

Abstract

As proposed at HB2010 [1], additional bunch-shape monitors have been installed at the last turns of the Injector 2 cyclotron and at several locations in the connecting beam line to the Ring cyclotron (@72 MeV), as well as behind the Ring cyclotron (@590 MeV). Now at each location in the beam lines, longitudinal-transversal 2D-density distributions of the bunched 2.2 mA proton beam can be taken from four angles of view, each separated by 45°. In addition the monitor in Injector 2 has been upgraded to observe the 13 outermost turns (@57 to 72 MeV), some of them from two or three angles of view. The measurement setup, data evaluation and results are outlined.

INTRODUCTION

The arrival time of protons, scattered at a 33 μm diameter carbon wire under 90° towards a scintillator-photomultiplier (PMT) detector, is measured with respect to the accelerator radio-frequency (50.63 MHz) reference phase. The histogram sampled over a large number of bunches represents the longitudinal density distribution of the bunches at the wire position. Repetition at several transversal positions delivers a two-dimensional (2D) projected profile of the charge density of the bunch.

NEW DETECTOR SETUP

In the cyclotrons and beam lines (Fig. 1) different detector configurations are used (Fig. 2). Multiple wires provide longitudinal-transversal 2D-density distributions from more than one angle of view.

More relays have been added to the timing circuit described in Ref. [1], allowing the single unit to be used for all detectors.

The time resolution can be determined by measuring the distribution of the differences of arrival times of each proton at two detectors. In contrast to Ref. [2], where the method is based on separate scintillators and PMTs, here both pairs of anodes of a four-anode PMT (Hamamatsu R7600U-200-M4) at a single scintillator are used. (For standard operation all four anodes are combined.) First tests indicate, that the time resolution of the old and new detectors are roughly the same. This is somewhat surprising since more photo-electrons should be created at the PMT anodes due to the truncated-pyramide shape and the higher light yield of the new scintillator (BC418) and the higher quantum efficiency of the new PMT.

The new shape also allows the use of a larger aperture (8 mm x 8 mm) in front of the scintillator. The count rate is consequently increased, and the time for sampling a 2D projected profile at the beam line reduces to typically 6 minutes.

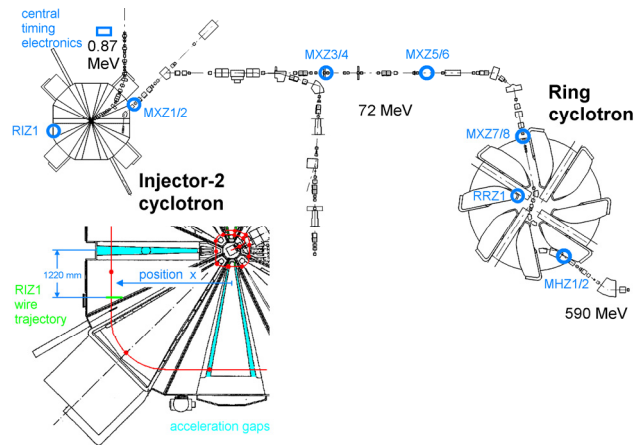


Figure 1: Locations of bunch-shape measurements.

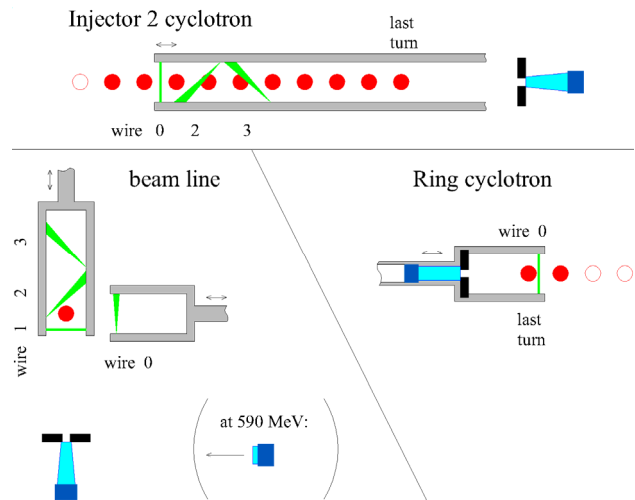


Figure 2: Orientation of beam, wires, drives, scintillators and PMTs (seen in beam direction). Most wires are tilted 45° in beam direction (schematic; the broader printed wire ends are closer to the beholder). Wire centers and scintillator axis are in one plane transversal to the beam. Only in Injector 2 can several wires be in the beam at the same time.

At the 590 MeV location, the deflected protons of 475 MeV are not stopped in the scintillator. Hence, contrary to the situation at 72 MeV, the highest pulses result not from the elastically scattered protons. However, a defined upper pulse height exists, hence allowing the same pulse selection scheme of Ref. [1], which uses only the highest pulses, to be used. Nevertheless, a smaller scintillator (3.7 mm x 3.7 mm x 18 mm) was needed, in order to limit the anode current of the PMT to below critical values.

MEASUREMENT AND EVALUATION PROCEDURE

In the Cyclotrons

The increasing bunch speed in the cyclotrons requires a more refined measurement and evaluation scheme which is delineated in the following case of Injector 2.

In the Injector 2 cyclotron the bunch trajectory per turn consists of four bends in the sector magnets and four nearly straight sections in between. With x [m] the minimum distance of a straight section to the machine center, $k = 1.1653$ reflecting the turn shape, $N = 10$ the harmonic number of the cyclotron, $t_{RF} = 19.75$ ns the RF period, c the speed of light, the relativistic β_{\parallel} corresponding to the bunch velocity increases during acceleration as $\beta_{\parallel} = k 2\pi x / (c N t_{RF}) = 0.12366 x$.

The deflection by 90° at a C_{12} atom of the scanning wire by a single elastic scattering event reduces the speed to $\beta_{\perp} = \beta_{\parallel} \sqrt{1 - M^2} / \left(1 + M \sqrt{1 - \beta_{\parallel}^2}\right)$ with $M = 1/11.91$ the ratio of rest mass of the proton m_{op} and the rest mass of the carbon nucleus. The proton kinetic energy then amounts to $W_{\perp} = m_{op} c^2 \left(\left(1 / \sqrt{1 - \beta_{\perp}^2}\right) - 1 \right)$.

The travel time of the scattered proton from the wire at a (as above defined) momentary position x to the detector at position x_{det} is $\Delta t = (x_{det} - x) / (\beta_{\perp} c)$. It is corrected for by subtraction.

The light output of the scintillator increases approximately proportionally to the proton kinetic energy W_{\perp} [3]. Since the leading edge discriminator level is fixed, the PMT output pulse height must be kept constant in order to prevent discriminator walk, and to still just trigger only at the highest pulses generated by the elastically scattered protons. To provide this compensation, the PMT voltage U_{PMT} is increased during the measurement at smaller x

according to $U_{PMT} = U_{PMT,ref} (W_{\perp,ref} / W_{\perp})^{1/b}$, with $U_{PMT,ref}$ empirically determined at a reference position x_{ref} with scattered proton energy $W_{\perp,ref}$. The exponent b describes the PMT gain as a function of PMT voltage: $gain / gain_{ref} = (U_{PMT} / U_{PMT,ref})^b$. According to Ref. [4] it is approximately $b = 8.7$ for the Hamamatsu R7600U-M4-200 used in the Injector 2. Empirically we find better results with $b = 7.0$. With this value, the ratio of a small fraction of non-suppressed inelastic scattering events to the bulk of the elastically scattered stays approximately constant over all turns. (We have not confirmed this number by checking the gain-voltage dependency of the PMTs directly.) In the Ring cyclotron, with only two turns visible, this correction is not applied.

With the variation of the distance $x_{det} - x$, also the solid angle of the detector opening seen from the wire

changes. To compensate this, the local count rate is corrected by $(x_{det} - x)^2 / (x_{det} - x_{ref})^2$.

Furthermore, the cross section for a deflection by 90° at a C_{12} atom changes with β_{\parallel} . Rutherford scattering would roughly give a variation proportional to β_{\parallel}^4 . In fact, the dependency of cross section on β_{\parallel} seems to be stronger. Here a correction $(\beta_{\parallel} / \beta_{\parallel,ref})^{10}$ to the local count rate yields roughly the same integral counts for the bunches of all turns. This correction is more of a cosmetic nature, since the impact on the derived bunch parameters (moments) is negligible.

Figure 3 shows a measurement evaluated according to this scheme. To get the three angles of view, three scans must be performed at shifted PMT voltage ramps (Fig. 4).

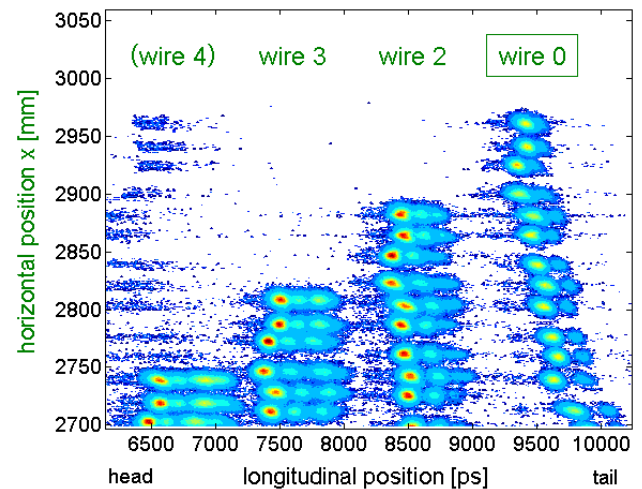


Figure 3: Result of one scan in the Injector 2. The position of vertical wire 0 is shown to the left. The probe arm moves horizontally, perpendicular to the straight trajectory of the bunches between the separated sector magnets. The diagonal wires 2, 3 and the wire 4 for the old detector are separated 75 mm each. PMT voltage and corrections at evaluation fit only to wire 0. The time scale is adapted to roughly show a picture “as seen from above” (but this doesn’t account for the bunch velocity increasing with turn number). The PMT voltage ramp is set just high enough that all elastically scattered protons reaching the scintillator are detected. Since the pulse height resolution is not good enough in the environment of the cyclotron, a “shadow bunch” resulting from inelastic scattering is already visible to the right. (At the other wires, where the PMT voltage is much too high, more “shadow bunches” are visible from inelastic scattering with higher energy loss.) The lower signal of the elastic scattered protons of wire 0 compared to wire 2-4 results from the fact that wire 0 is the only one not inclined in beam direction.

We have to mention, that the assumed linear increase of the longitudinal proton velocity with the horizontal position x is not strictly given. On the one hand, the horizontal betatron oscillation leads to a deviation. On the

other hand, the space-charge driven “roll-up” mechanism, which creates the short bunches in Injector 2 [5], probably leads to a less than linear velocity increase inside a bunch. If this is the case, the parameters derived for a bunch, i.e. transversal-longitudinal correlation and transversal and longitudinal moments, would change significantly. A constant longitudinal proton velocity inside a bunch may

be the better assumption, when producing data for “Transport”-like simulation codes. Anyhow, for comparison with detailed beam dynamics simulations, this source of error can be eliminated by implementing the 90° scattering and the travel towards the detector into the simulation in order to directly compare simulated with measured time distributions at the detector.

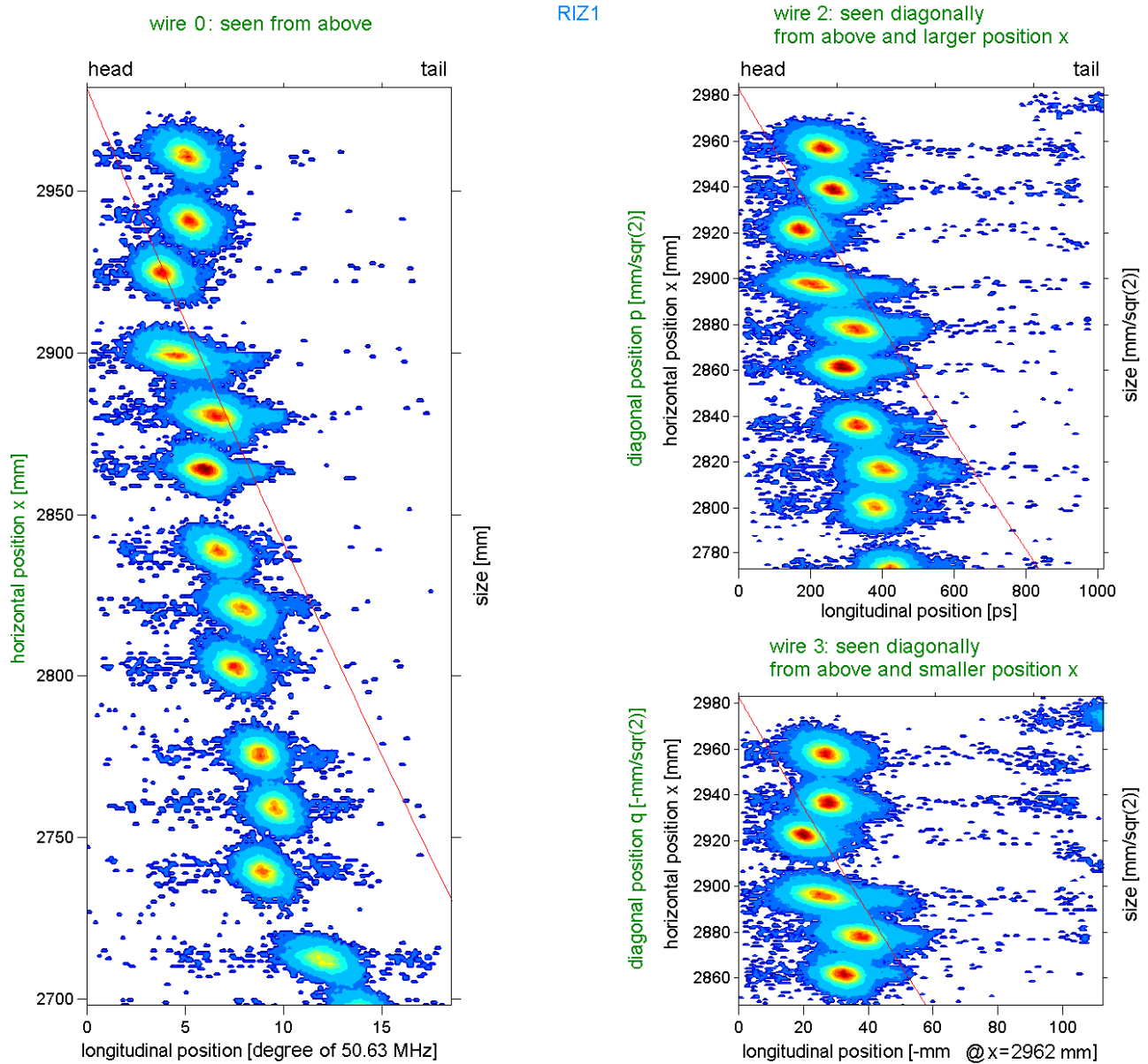


Figure 4: Result of three separate scans in the Injector 2 with correspondingly adapted PMT voltage ramps (voltage travel ~ 17 V). Compared to Fig. 3 relatively lower PMT voltages (by 3 V) are used, giving just nearly negligible “shadow bunches”. On the other hand, the elastic peaks are not fully developed, i.e. having different count sums. The smallest voltage step of 1 V, provided by the high voltage supply, results already in visible discontinuities at the 4th to 6th last turns “shadow bunches”. The red line indicates isochronicity. A relative phase slip of $\sim 9^\circ$ builds up over the last 11 turns. Taken at production beam current of ~ 2200 μ A. Longitudinal scales are identical. Contour levels every 10% and at 1% and 0.1%. (The 10%-level is given by the border between cyan and light blue.)

In the Beam Lines

At the present evaluation of measurements at the beam line, the longitudinal velocity distribution of the protons in the bunch is ignored by assuming a proton energy of 72 MeV. A longitudinal scale in mm is given accordingly. This is in the same respect not fully correct.

MEASUREMENT RESULTS

Figure 4 depicts the bunches at the last 13 turns in the Injector 2 cyclotron. The bunch size is roughly that of a vertically compressed cherry and stays quite constant over the visible turns. The projections are very close to a Gaussian.

Along the transfer line and in the Ring cyclotron the bunch length increases and non-ellipsoidal bunch shapes evolve (Fig. 5).

At the location inside the Ring cyclotron, the detector shielding against x-rays from the extraction elements has been improved, and the background was largely reduced.

Nevertheless, the background noise is partially created by protons which are scattered at the carbon wire and lost e.g. at the extraction elements. The phase of x-rays from the extraction elements, arriving at the given detector location, is, by chance, similar to the one of the 90° scattered protons. Hence, it is still difficult to judge how much the bunch shape is affected by this background.

At the location MXZ1/2 shortly after Injector 2, the bunch is horizontally extremely narrow. Hence the wire 0 does not survive at full (production) beam current.

The size of the bunches in Injector 2 shrinks with the beam current [2]. This gets also visible shortly after extraction at MXZ1/2. Figure 6 depicts two measurements at a small beam current with extremely short bunches. The bunch length gets comparable with the time resolution of the detector ($\sigma_{\text{det}} \cong 13.5$ ps). The measured time distribution is corrected for the detector resolution, but as Fig. 6 illustrates, this technique reaches its limits here.

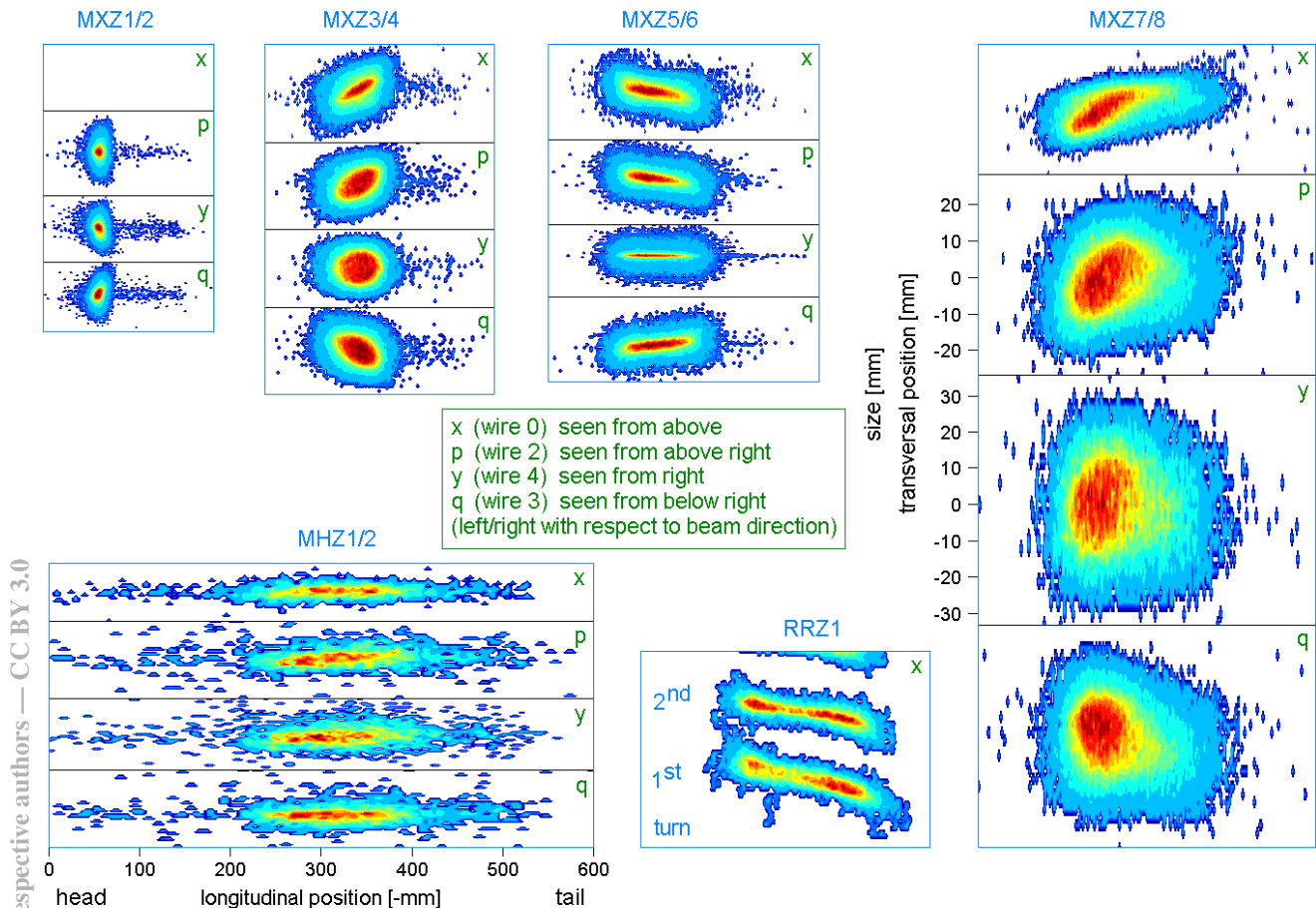


Figure 5: Measured 2D projections along the 72 MeV transfer line, the first two turns of the Ring cyclotron and at its exit at 590 MeV (clockwise from above left). Taken at production beam current of ~ 2200 μA . Transversal scales x, p, y, q are all identical. The longitudinal scales are compressed by a factor of 4 respectively. The trailing particles behind the short bunches (MXZ1-6) are assumed to be an instrument effect. Background suppression is employed at RR1. MHZ1/2 suffers from low count sum.

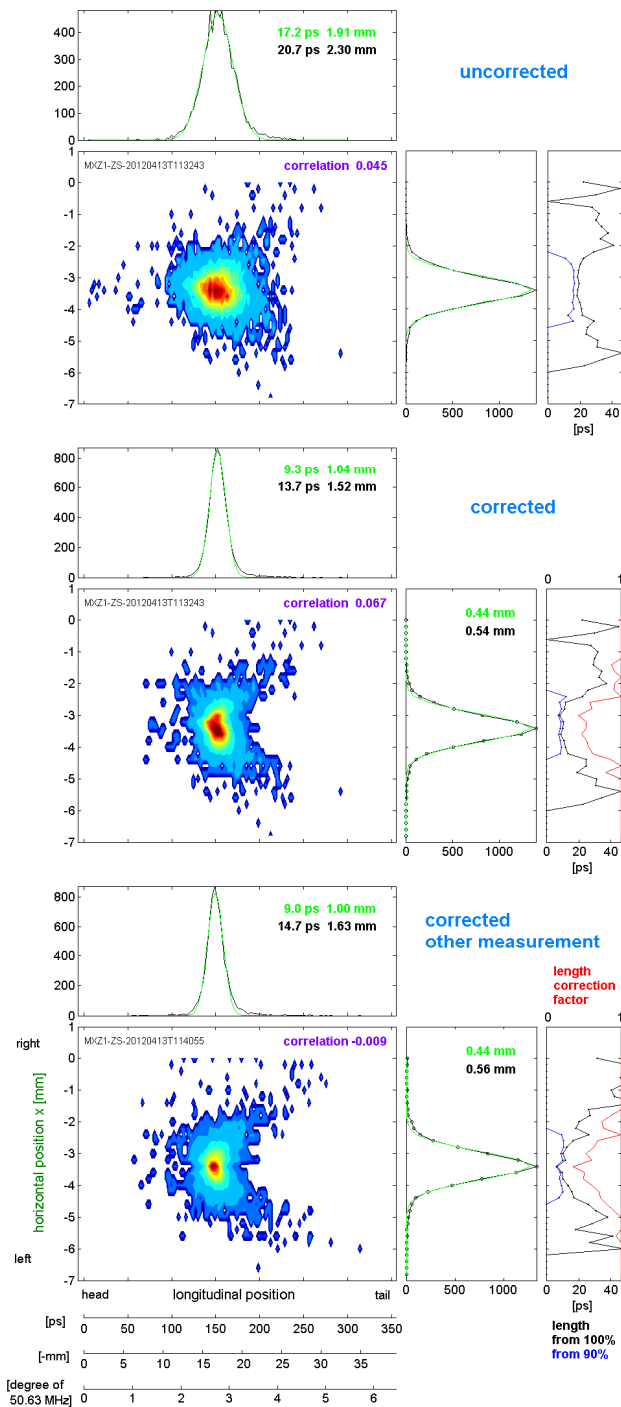


Figure 6: Measured 2D projections shortly after extraction of Injector 2 (MXZ1/2) at a beam current of only 50 μA . First scan shown without (above) and with (middle) correction for detector time resolution. Second scan (below) taken subsequently at same conditions. 1σ values from second moments (black) and Gaussian fits (green) are given for the projections. For the local width of the local full and 90%-core distribution, 1σ values from Gaussian fits are displayed to the right. Also the shortening by the local correction is indicated (red).

The correction is performed locally, i.e. at each wire position, by shrinking the measured local time distribution around its centre by the factor $\sqrt{1 - (\sigma_{\text{det}}^2 / \sigma_{\text{meas}}^2)}$ (quadratic subtraction). σ_{meas} is derived from a fit with a Gaussian and not from the second moment, to give some immunity against background. The correction is only performed if a useful fit is found.

OUTLOOK

As outlined in Ref. [1], for a better understanding of beam losses, detailed numerical simulations of the beam transport and matching including the beam halo are required *together* with *detailed* measurements of the beam distributions. Together with wire monitors, loss monitors and possibly other monitors, the bunch-shape measurements can deliver detailed information on the bunch density distribution. On the one hand, it is still needed to improve the quality of the measurements and error estimations. On the other hand, not only many machine details have to be included into the simulation, also the ability of simulation codes to find an initial distribution, fitting best to all these measurements and its errors, needs to be improved [6].

ACKNOWLEDGMENTS

The author would like to thank M. Rohrer and D. Hauenstein for the elaboration of the mechanical design, R. Erne for assembling, G. Gamma for MEMS tests and PMT base production, U. Frei and E. Johansen for providing motor-driving units and firmware.

REFERENCES

- [1] R. Dölling, “Bunch Shape Measurements at Injector 2 and Ring Cyclotron”, HB2010, Morschach, September 2010, MOPD62, p. 235 (2010); <http://www.JACoW.org>.
- [2] R. Dölling, “Measurement of the Time-Structure of the 72-MeV Proton Beam in the PSI Injector-2 Cyclotron”, DIPAC01, Grenoble, May 2001, PS05, p. 111 (2001); <http://www.JACoW.org>.
- [3] “BC-418, BC-420, BC-422 datasheet”, (2005), <http://www.detectors.saint-gobain.com/>.
- [4] HAMAMATSU Photonics, personal communication.
- [5] J. J. Yang, A. Adelman, M. Humbel, M. Seidel, T. J. Zhang, “Beam Dynamics in High Intensity Cyclotrons including Neighboring Bunch Effects: Model, Implementation, and Application”, Phys. Rev. ST Accel. Beams 13, 064201 (2010).
- [6] Y. Ineichen, A. Adelman, C. Bekas, A. Curioni, P. Arbenz, “A Fast and Scalable Low Dimensional Solver for Charged Particle Dynamics in Large Particle Accelerators”, Comput. Sci. Res. Dev. 27 (2012), doi:10.1007/s00450-012-0216-2.